

Effect of Structural Parameters on Superconductivity in Fluorine-Free LnFeAsO_{1-y} ($\text{Ln}=\text{La}, \text{Nd}$)

Chul-Ho LEE, Akira IYO, Hiroshi EISAKI, Hijiri KITO, Maria Teresa FERNANDEZ-DIAZ¹, Toshimitsu ITO, Kunihiro KIHOU, Hirofumi MATSUHATA, Markus BRADEN², and Kazuyoshi YAMADA³

National Institute of Advanced Industrial Science and Technology, Tsukuba, Ibaraki 305-8568, Japan

¹*Institut Laue-Langevin, BP 156, F-38042 Grenoble Cedex 9, France*

²*II. Physikalisches Institut, Universität zu Köln, Zùlpicher Str. 77, D-50937 Köln, Germany*

³*Institute for Materials Research, Tohoku University, Sendai 980-8577, Japan*

The crystal structure of LnFeAsO_{1-y} ($\text{Ln} = \text{La}, \text{Nd}$) has been studied by the powder neutron diffraction technique. The superconducting phase diagram of NdFeAsO_{1-y} is established as a function of oxygen content which is determined by Rietveld refinement. The small As-Fe bond length suggests that As and Fe atoms are connected covalently. FeAs_4 -tetrahedrons transform toward a regular shape with increasing oxygen deficiency. Superconducting transition temperatures seem to attain maximum values for regular FeAs_4 -tetrahedrons.

KEYWORDS: oxypnictides, superconductivity, powder neutron diffraction, crystal structure analysis

The recent discovery of superconductivity in $\text{LaFeAsO}_{1-x}\text{F}_x$ with a transition temperature of $T_c = 26$ K has triggered an intense search for related new superconductors.¹ Immediately, it was found that T_c increases up to 55 K by replacing La with Sm atoms.² This is the highest T_c besides that in high- T_c cuprates rendering oxypnictides a promising new class of superconductors.

Because the T_c of the oxypnictide superconductors is very high, it may be difficult to explain the formation of Cooper pairs with the conventional BCS theory. Replacing As by the lighter P results in a strong suppression of the T_c in $\text{LaFePO}_{1-x}\text{F}_x$,³ whose origin also needs to be explained. To elucidate the superconducting mechanism, information about the crystal structure of these materials is very important.

The parent compounds of LnFeAsO ($\text{Ln} = \text{lanthanide}$) exhibit a tetragonal structure with the space group $P4/\text{mmm}$ at room temperature⁴ (Fig. 1). Characteristically, LnO and FeAs layers are stacked alternately. Fe atoms are in a four-fold coordination forming a FeAs_4 -tetrahedron. Upon doping, LnO layers provide carriers to FeAs layers where superconductivity is expected to be induced. The function of the layers appears clearly separated similarly to high- T_c cuprates.

Very recently, it has been reported that the fluorine-free samples LnFeAsO_{1-y} show superconductivity with a maximum T_c of 55 K, as well.^{5,6} Based on the nominal composition, superconductivity appears to be induced in a wide range of oxygen deficiencies, $0.3 \leq y \leq 0.8$. Since the oxygen deficiency is huge, the crystal structure could be significantly modified compared with that of the parent LnFeAsO compounds. Furthermore, one may doubt that the real oxygen deficiency is as large as the nominal values. Neutron diffraction measurements on the LnFeAsO_{1-y} samples are required to confirm the crystal structure as well as the oxygen content. In this study, we report the relationship between superconductivity and crystal structure in LnFeAsO_{1-y} compounds.

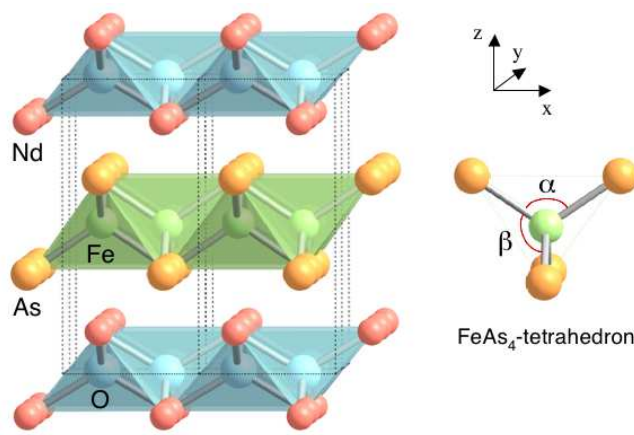


Fig. 1. Crystal structure of NdFeAsO . Dashed lines show unit cells. NdO and FeAs layers are stacked alternately. FeAs_4 clusters in the FeAs layers form a tetrahedral lattice. The definitions of the two As-Fe-As bond angles α and β are illustrated on the right side with an FeAs_4 -tetrahedron.

Polycrystalline samples of LnFeAsO_{1-y} ($\text{Ln}=\text{La}, \text{Nd}$) were synthesized at high pressure and high temperature using a cubic-anvil high-pressure apparatus. Details of synthesis method are given in ref. 5. The nominal oxygen deficiencies at the start of the synthesis was $y = 0.15, 0.20, 0.30$, and 0.40 in the NdFeAsO_{1-y} samples labeled 1, 2, 3, and 4. For a LaFeAsO_{1-y} sample, the nominal content is $y = 0.40$ (sample 5). The oxygen composition of all the samples was determined by the present Rietveld analysis, and we found that it largely shifts towards higher oxidation, see Table 1. The amount of samples used was about 0.5 g for each composition.

The T_c of the LnFeAsO_{1-y} ($\text{Ln}=\text{La}, \text{Nd}$) samples was measured using a SQUID magnetometer under a magnetic field of 5 Oe after zero field cooling from sufficiently above T_c (Fig. 2). The oxygen deficiency y indicated in Fig. 2 corresponds to that obtained from the Rietveld analysis of the neutron diffraction patterns. The T_c val-

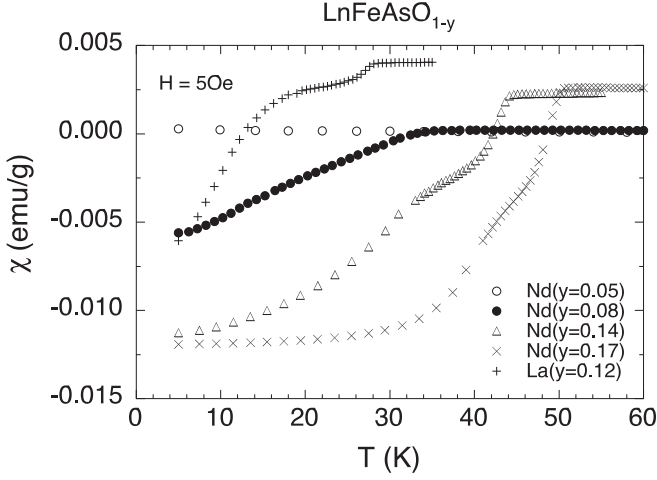


Fig. 2. Shielding signals of LnFeAsO_{1-y} measured under a magnetic field of $H = 50$ Oe. y was determined by Rietveld refinement. The higher values in the normal states of LaFeAsO_{1-y} ($y = 0.12$) and NdFeAsO_{1-y} ($y = 0.14, 0.17$) could be due to slight impurities of iron compounds.

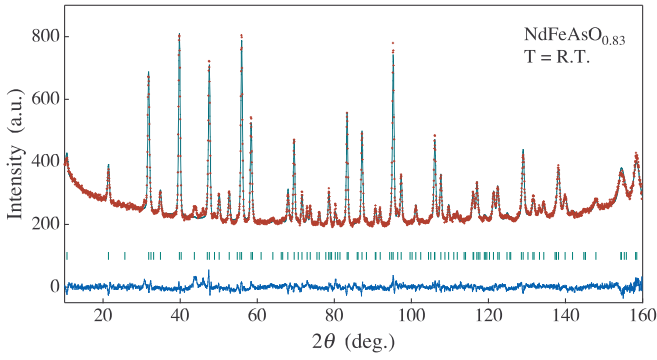


Fig. 3. Typical observed (crosses) and calculated (solid lines) neutron powder diffraction patterns of NdFeAsO_{1-y} . Vertical bars show the calculated positions of nuclear Bragg reflections. The solid lines shown at the bottom of the figure indicate the differences between observations and calculations.

ues of the La-based, $y = 0.12$, and of the Nd-based, $y = 0.08, 0.14$, and 0.17 , samples are 28 K, 35 K, 44 K, and 51 K, respectively. On the other hand, the Nd-based sample with $y = 0.05$ sample is not superconducting.

Neutron scattering measurement was carried out using the high-resolution powder diffractometer D2B of the Institut Laue-Langevin in Grenoble, France. Incident neutron wavelength was fixed at 1.594 \AA using a Ge monochromator. Diffraction patterns were collected in the 2θ range of 9° - 160° at a constant step of 0.05° using a multidetector. Powder samples were placed in a cylindrical vanadium can for measurements at room temperature. These vanadium cans were mounted in a closed-cycle cryostat for measurements at $T = 10 \text{ K}$. The data were analyzed by the Rietveld method using the Rietan program¹⁰ for the refinement of crystallographic structures.

Figure 3 shows a typical diffraction pattern of $\text{NdFeAsO}_{0.83}$. Small amounts of the impurity phases, LaAs , NdAs , FeAs , La_2O_3 , and Nd_2O_3 exist in the series of measurements with a volume ratio of about

Table I. Atomic parameters of LnFeAsO_{1-y} (space group $P4/nmm$) determined by Rietveld refinements of neutron powder diffraction data. B is the isotropic atomic displacement parameter.

Atom	site	occ.	x	y	z	$B \text{ (\AA}^2\text{)}$
(a) sample 1 (non-super) $T = \text{R.T.}$						
$a = 3.96666(7) \text{ \AA}$, $c = 8.5699(2) \text{ \AA}$, $R_{WP} = 2.98 \%$						
Nd	2c	1	1/4	1/4	0.1390(2)	0.46(4)
Fe	2b	1	3/4	1/4	0.5	0.57(4)
As	2c	1	1/4	1/4	0.6571(3)	0.50(5)
O	2a	0.95(1)	3/4	1/4	0	0.49(8)
(b) sample 2 ($T_c = 35 \text{ K}$) $T = \text{R.T.}$						
$a = 3.95940(6) \text{ \AA}$, $c = 8.5550(2) \text{ \AA}$, $R_{WP} = 2.66 \%$						
Nd	2c	1	1/4	1/4	0.1413(2)	0.34(3)
Fe	2b	1	3/4	1/4	0.5	0.42(3)
As	2c	1	1/4	1/4	0.6586(3)	0.53(4)
O	2a	0.920(9)	3/4	1/4	0	0.67(7)
(c) sample 3 ($T_c = 44 \text{ K}$) $T = \text{R.T.}$						
$a = 3.95365(7) \text{ \AA}$, $c = 8.5581(2) \text{ \AA}$, $R_{WP} = 3.25 \%$						
Nd	2c	1	1/4	1/4	0.1429(3)	0.23(4)
Fe	2b	1	3/4	1/4	0.5	0.37(4)
As	2c	1	1/4	1/4	0.6587(3)	0.39(5)
O	2a	0.86(1)	3/4	1/4	0	0.32(8)
(d) sample 4 ($T_c = 51 \text{ K}$) $T = \text{R.T.}$						
$a = 3.94755(7) \text{ \AA}$, $c = 8.5446(2) \text{ \AA}$, $R_{WP} = 2.84 \%$						
Nd	2c	1	1/4	1/4	0.1440(3)	0.42(4)
Fe	2b	1	3/4	1/4	0.5	0.40(3)
As	2c	1	1/4	1/4	0.6600(3)	0.41(5)
O	2a	0.83(1)	3/4	1/4	0	0.66(8)
(e) sample 4 ($T_c = 51 \text{ K}$) $T = 10 \text{ K}$						
$a = 3.9423(1) \text{ \AA}$, $c = 8.5129(3) \text{ \AA}$, $R_{WP} = 4.07 \%$						
Nd	2c	1	1/4	1/4	0.1434(3)	0.46(6)
Fe	2b	1	3/4	1/4	0.5	0.49(5)
As	2c	1	1/4	1/4	0.6624(4)	0.36(6)
O	2a	0.83	3/4	1/4	0	0.48(9)
(f) sample 5 ($T_c = 28 \text{ K}$) $T = \text{R.T.}$						
$a = 4.02291(8) \text{ \AA}$, $c = 8.7121(2) \text{ \AA}$, $R_{WP} = 3.87 \%$						
La	2c	1	1/4	1/4	0.1453(3)	0.38(5)
Fe	2b	1	3/4	1/4	0.5	0.27(4)
As	2c	1	1/4	1/4	0.6527(4)	0.41(6)
O	2a	0.88(1)	3/4	1/4	0	0.54(9)

3% at most. The space group $P4/nmm$ was assumed for all calculations; it has been confirmed recently by the electron diffraction study on superconducting NdFeAsO_{1-y} .⁷ Since the oxygen content of the synthesized samples can deviate from that of the starting materials, the occupation of the oxygen site was varied in the refinements. The obtained R factors were in the range of $2.66 \% \leq R_{WP} \leq 4.07 \%$ (Table 1). The R factor for $\text{NdFeAsO}_{0.83}$ (sample 4) at $T = 10 \text{ K}$ is slightly larger owing to some contamination in the diffraction pattern through the cryostat. It turned out that the actual oxygen contents of the samples are larger than the nominal (intended) values for all the samples used in the current experiments. This is due to the oxidation of the starting rare-earth elements.

The superconducting phase diagram of NdFeAsO_{1-y} versus the oxygen deficiency y determined by Rietveld analysis is shown in Fig. 4. The superconductivity appears above $y = 0.05$ and attains a maximum T_c value for

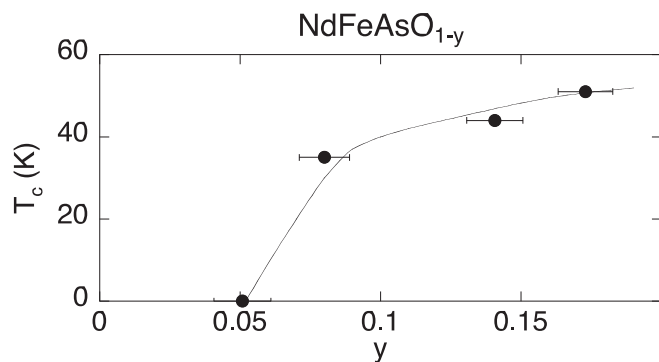


Fig. 4. T_c vs oxygen deficiency y in NdFeAsO_{1-y} .

NdFeAsO_{1-y} compounds around $y = 0.17$. The phase diagram is similar to that of the recently reported fluorine-doped $\text{NdFeAsO}_{1-x}\text{F}_x$ ¹¹ which suggests an equivalent carrier doping level when the y and x values are the same, although the amount of induced carriers should be two times larger for oxygen deficiency.

The selected crystal structural parameters obtained from the Rietveld analysis are shown in Fig. 5. For the non-doped LaFeAsO , the parameters were extracted from the literature.⁸ Ln-O bond length increases with increasing oxygen deficiency at the same rate in LaFeAsO_{1-y} and NdFeAsO_{1-y} , possibly owing to the decrease in the number of electrons in the O-planes. The bond lengths may be analyzed by the bond-valence-sum (BVS) formalism,¹²⁻¹⁴ in which each bond with a distance r contributes a valence $v = \exp[\frac{(d-r)}{0.37}]$ with d as an empirical parameter. In the non-superconducting $\text{NdFeAsO}_{0.95}$, the four Nd-O bonds contribute 2.235 to the Nd-BVS after correction for the incomplete oxygen occupation. In contrast, the four Nd-As bonds, which are significantly longer, contribute only 0.870 to the Nd-BVS which demonstrates the very anisotropic bonding of the Nd coordination. The total Nd-BVS is 3.104 in good agreement with the expected Nd valency. The increase in Ln-O bond length with doping strongly reduces the Nd-O contribution to the Nd-BVS to 1.888 for $y=0.17$. This reduction is only partially compensated through the pronounced shrinking of Nd-As distance with doping. For $y=0.17$, the Nd-As bonds contribute 0.994 to the Nd-BVS resulting in a total Nd-BVS value of 2.882, which is still close to the expected value. In contrast, the BVS at the Fe site is doping-independent and always far above the value expected for an ionic picture; $\text{Fe-BVS}=3.522$ for $y=0.05$ and 3.485 for $y=0.17$. The enhanced BVS directly indicates that Fe-As bonds are too short compared with an ionic picture and strongly suggests a covalent bonding similar to the cuprates.¹²

The La and Nd series differ in doping dependence of the thickness of the FeAs layer, which is determined by the distance between the As sites and the plane through the Fe sites. This $\text{As-Fe}_{\text{plane}}$ distance increases more rapidly in the Nd-based compounds than in the La-based compounds. Related to this, the As-Fe-As bond angles of the Nd-based compounds vary more rapidly with increasing oxygen deficiency approaching a regular FeAs_4

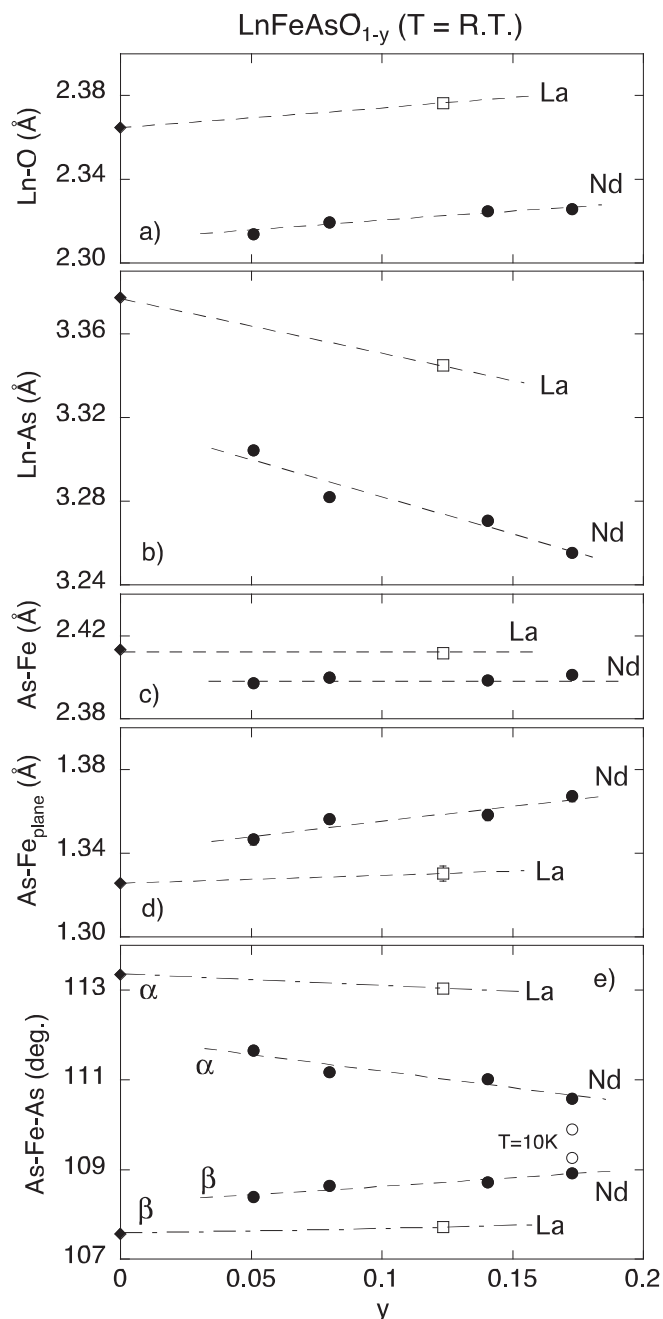


Fig. 5. Crystal structural parameters vs oxygen deficiency in LaFeAsO_{1-y} at room temperature (open squares), NdFeAsO_{1-y} at room temperature (closed circles), and NdFeAsO_{1-y} at $T = 10\text{K}$ (open circles). The data of LaFeAsO (closed diamond) is cited from the literature.⁸ The bond length of (a) Nd-O, (b) Nd-As, (c) As-Fe, (d) distance between the Fe plane and the As atom, and (e) As-Fe-As bond angles are depicted. The definitions of the bond angles α and β are illustrated in Fig. 1.

tetrahedron in which α and β are 109.47° . Also upon cooling, the FeAs_4 -tetrahedrons become more regular.

The relationship between T_c and FeAs_4 -tetrahedral distortion is shown in Fig. 6. The tetrahedral distortion is represented by the As-Fe-As bond angle. Clearly, T_c increases as the FeAs_4 coordination becomes a regular tetrahedron. This suggests that the maximum T_c values are attained when the FeAs_4 -lattices form a regular tetrahedron. This tendency could not change by lower-

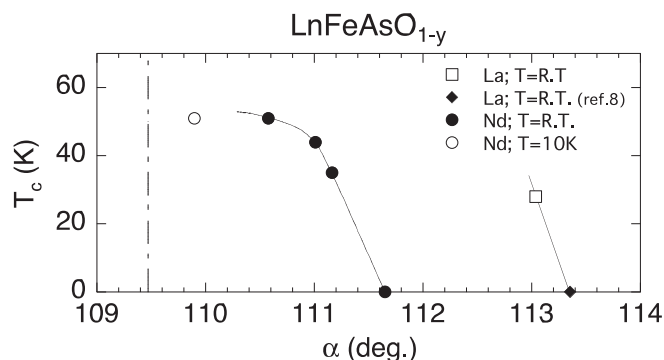


Fig. 6. Relationship between T_c and FeAs_4 -tetrahedral distortion in LaFeAsO_{1-y} at room temperature (open square), NdFeAsO_{1-y} at room temperature (closed circles), and NdFeAsO_{1-y} at $T = 10\text{K}$ (open circle). The value of LaFeAsO (closed diamond) was taken from ref. 8. The definition of As-Fe-As bond angle α is illustrated in Fig. 1. The vertical dashed line indicates the bond angle of a regular tetrahedron ($\alpha = 109.47^\circ$).

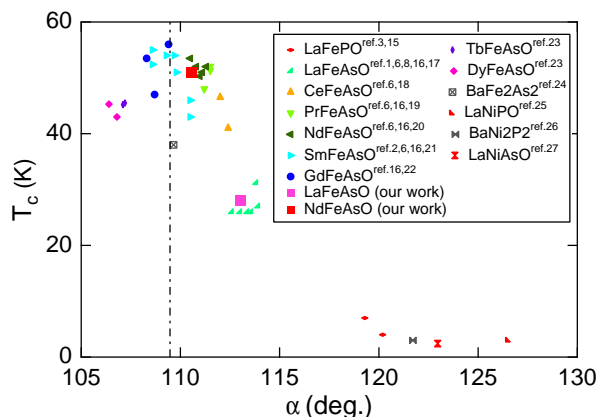


Fig. 7. T_c vs As-Fe-As bond angle α for various pnictide superconductors. Formulas of parent compositions of superconductors are depicted in the inset. Crystal structure parameters of samples showing almost maximum T_c in each system are selected. The vertical dashed line indicates the bond angle of a regular tetrahedron ($\alpha = 109.47^\circ$).

ing temperature, since they become closer to a regular tetrahedron at $T = 10\text{ K}$ for the sample showing the highest T_c . To confirm this idea, we show in Fig. 7 As-Fe-As bond angle as a function of T_c in various pnictide superconductors.^{1-3, 6, 8, 15-27} The parameters of the samples showing almost maximum T_c in each system are selected to eliminate the effect of carrier doping. The As-Fe-As bond angles in several LnFeAsO_{1-y} compounds were estimated from the lattice constants assuming a constant As-Fe bond length of 2.40 \AA . This assumption is supported by the present results which suggest that the rare-earth dependence of As-Fe bond length is small. This estimation can cause a bond-angle error of about 1° . Clearly, T_c becomes maximum when FeAs_4 -lattices form a regular tetrahedron. This result indicates a clear relationship between crystal structure and superconductivity.

In summary, we have studied the crystal structure of $(\text{La}, \text{Nd})\text{FeAsO}_{1-y}$ by the neutron diffraction technique.

Rietveld analysis revealed that the real oxygen content is largely above the nominal composition. We present the superconducting phase diagram of NdFeAsO_{1-y} against the actual oxygen content. FeAs_4 -lattices were transformed toward a regular tetrahedron accompanied by an increase in T_c with increasing oxygen deficiency y . It seems that T_c becomes maximum when the FeAs_4 -lattices form a regular tetrahedron.

Acknowledgments

The authors would like to thank K. Kuroki, H. Aoki, R. Arita, K. Terakura, S. Ishibashi, I. Hase, N. Takeshita, K. Miyazawa, P. M. Shirage, and R. Kumai for valuable discussions and the ILL for beam time allocation. This work was supported by Grants-in-Aid for Scientific Research on Priority Areas and for Scientific Research B (No. 19340106) from MEXT, Japan, and performed under the interuniversity cooperative research program of the Institute for Materials Research, Tohoku University. Work in Cologne was supported by the DFG through SFB608.

- 1) Y. Kamihara, T. Watanabe, M. Hirano, and H. Hosono: J. Am. Chem. Soc. **130** (2008) 3296.
- 2) Z. A. Ren, W. Lu, J. Yang, W. Yi, X. L. Shen, Z. C. Li, G. C. Che, X. L. Dong, L. L. Sun, F. Zhou, and Z. X. Zhao: Chin. Phys. Lett. **25** (2008) 2215.
- 3) Y. Kamihara, H. Hiramatsu, M. Hirano, R. Kawamura, H. Yanagi, T. Kamiya, and H. Hosono: J. Am. Chem. Soc. **128** (2006) 10012.
- 4) P. Quebe, L. J. Terbüchte, and W. Jeitschko: J. Alloys Comp. **302** (2008) 70.
- 5) H. Kito, H. Eisaki, and A. Iyo: J. Phys. Soc. Jpn. **77** (2008) 063707.
- 6) Z. A. Ren, G. C. Che, X. L. Dong, J. Yang, W. Lu, W. Yi, X. L. Shen, Z. C. Li, L. L. Sun, F. Zhou, and Z. X. Zhao: Europhys. Lett. **83** (2008) 17002.
- 7) H. Matsuhata: private communication.
- 8) T. Nomura, S. W. Kim, Y. Kamihara, M. Hirano, P. V. Sushko, K. Kato, M. Takata, A. L. Shluger, and H. Hosono: cond-mat: 0804.3569.
- 9) C. de la Cruz, Q. Huang, J. W. Jynn, J. Li, W. Ratcliff II, J. L. Zarestky, H. A. Mook, G. F. Chen, J. L. Luo, N. L. Wang, and P. Dai: to be published in Nature (2008).
- 10) F. Izumi and T. Ikeda: Mater. Sci. Forum **321-324** (2000) 198.
- 11) G. F. Chen, Z. Li, D. Wu, J. Dong, G. Li, W. Z. Hu, P. Zheng, J. L. Luo, and N. L. Wang: cond-mat: 0803.4384v1.
- 12) B. Cordero, V. Gómez, A. E. Platero-Prats, M. Revés, J. Echeverría, E. Cremades, F. Barragán, and S. Alvarez: Dalton Trans. (2008) 2832.
- 13) R. D. Shannon: Acta Cryst. **A32** (1976) 751.
- 14) N.E. Brese and M. O'Kneefe: Acta Cryst. **B47** (1991) 192.
- 15) M. Tegel, I. Schellenberg, R. Pöttgen, and D. Johrendt: cond-mat: 0805.1208.
- 16) A. Iyo: private communication.
- 17) Y. Qiu, M. Kofu, Wei Bao, S. H. Lee, Q. Huang, T. Yildirim, J. R. D. Copley, J. W. Lynn, T. Wu, G. Wu, and X. H. Chen: cond-mat: 0805.1062.
- 18) G. F. Chen, Z. Li, D. Wu, G. Li, W. Z. Hu, J. Dong, P. Zheng, J. L. Luo, and N. L. Wang: cond-mat: 0803.3790v3.
- 19) Z. A. Ren, J. Yang, W. Lu, W. Yi, G. C. Che, X. L. Dong, L. L. Sun, and Z. X. Zhao: cond-mat: 0803.4283.
- 20) X. L. Wang, R. Ghorbani, G. Peleckis, and S. X. Dou: cond-mat: 0806.0063v1; R. Kumai: private communication; Y. Jia, P. Cheng, L. Fang, H. Luo, H. Yang, C. Ren, L. Shan, C. Gu, and H. H. Wen: cond-mat: 0806.0532v1.
- 21) N. D. Zhigadlo, S. Katrych, Z. Bukowski, and J. Karpinski:

- cond-mat: 0806.0337; X. H. Chen, T. Wu, G. Wu, R. H. Liu, H. Chen, and D. F. Fang: cond-mat: 0803.3603; R. H. Liu, G. Wu, T. Wu, D. F. Fang, H. Chen, S. Y. Li, K. Liu, Y. L. Xie, X. F. Wang, R. L. Yang, L. Ding, C. He, D. L. Feng, and X. H. Chen: cond-mat: 0804.2105; C. Senatore, M. Cantoni, G. Wu, R.H. Liu, X.H. Chen, and R. Flukiger: cond-mat: 0805.2389; I. Felner, I. Nowik, M. I. Tsindlekht, Z. A. Ren, X. L. Shen, G. C. Che, and Z. X. Zao: cond-mat: 0805.2794.
- 22) J. Yang, Z. C. Li, W. Lu, W. Yi, X. L. Shen, Z. A. Ren, G. C. Che, X. L. Dong, L. L. Sun, F. Zhou, and Z. X. Zhao: Supercond. Sci. Technol. **21** (2008) 082001; C. Wang, L. Li, S. Chi, Z. Zhu, Z. Ren, Y. Li, Y. Wang, X. Lin, Y. Luo, S. Jiang, X. Xu, G. Cao, and Z. Xu: cond-mat: 0804.4290.
- 23) J. W. G. Bos, G. B. S. Penny, J. A. Rodgers, D. A. Sokolov, A. D. Huxley, and J. P. Attfield: cond-mat: 0806.0926.
- 24) M. Rotter, M. Tegel, and D. Johrendt: cond-mat: 0805.4630.
- 25) T. Watanabe, H. Yanagi, T. Kamiya, Y. Kamihara, H. Hiramatsu, M. Hirano, and H. Hosono: Inorg. Chem. **46** (2007) 7719.
- 26) V. Keimes, D. Johrendt, A. Mewis, C. Huhnt, and W. Schlabitz: Z. Anorg. Allg. Chem. **623** (1997) 1699; T. Mine, H. Yanagi, T. Kamiya, Y. Kamihara, M. Hirano, and H. Hosono: cond-mat: 0805.4305v1.
- 27) T. Watanabe, H. Yanagi, Y. Kamihara, T. Kamiya, M. Hirano, and H. Hosono: cond-mat: 0805.4340.